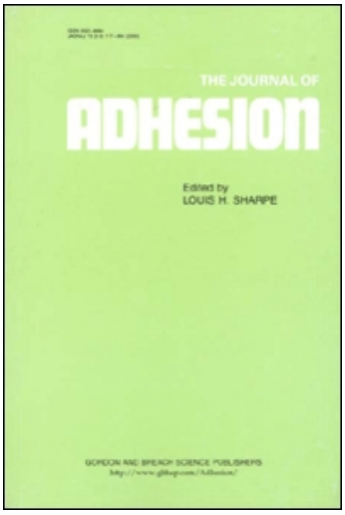

The Journal of Adhesion
Publication details, including instructions for authors and subscription information:
http://www.informaworld.com/smpp/title~content=t713453635

The Fiber/Matrix Bond Strength of CFRP Deduced from the Strength Transverse to the Fibers

P. W. M. Peters[a]
[a] DLR, Institut für Werkstoff-Forschung, Köln, Germany

To cite this Article Peters, P. W. M.(1995) 'The Fiber/Matrix Bond Strength of CFRP Deduced from the Strength Transverse to the Fibers', The Journal of Adhesion, 53: 1, 79 — 101
To link to this Article: DOI: 10.1080/00218469508014373
URL: http://dx.doi.org/10.1080/00218469508014373

J. Adhesion, 1995, Vol. 53, pp. 79–101
Reprints available directly from the publisher
Photocopying permitted by license only

The Fiber/Matrix Bond Strength of CFRP Deduced from the Strength Transverse to the Fibers*

P. W. M. PETERS

DLR, Institut für Werkstoff-Forschung, 51140 Köln, Germany

(Received March 26, 1994; in final form February 17, 1995)

The strength transverse to the fibre (or the transverse fracture strain) of CFRP is directly related to the fibre/matrix bond strength. This enables the determination of a fibre/matrix bond strength based on transverse fracture data. In crossply laminates, the transverse ply usually fails many times, so that principally these experiments deliver a treasure of data. A method, developed to make use of these data, produces a Weibull distribution for transverse fracture based on the data of, basically, a single specimen. A model developed to separate the influences of defects, matrix ductility and constraint finally leads to a procedure to determine the strain at interphase (or interface) failure. The usefulness of the model and the determined strain at interface failure is demonstrated with several examples, such as the influence of constraint, of test temperature and of the fibre surface treatment on transverse cracking and the fibre/matrix bond strength.

KEYWORDS: transverse crack; CFRP; Weibull distribution; interface; fibre/matrix bond strength

INTRODUCTION

The fibre/matrix bond strength is an important property which decisively influences the mechanical properties of fibre reinforced materials. The interaction of the fibre/matrix bond strength with matrix and fibre properties, resulting in a composite mechanical property, is in most cases complicated, so that it is very difficult to derive a bond strength from a mechanical property. For this reason, in the past years single-fibre composite samples were developed to study the phenomenon of fibre/matrix bonding. These techniques further are indispensable in the early stage of development of a fibre/matrix system, when preimpregnated fibre fabrics or preimpregnated unidirectionally-arranged fibres are not available. Most important single fibre composite techniques are, *e.g.*, the single-fibre multifragmentation and single-fibre pull-out test. Classical fundamental studies on the fibre/matrix bond strength in CFRP were performed by Drzal *et al.*,[1, 2, 3] making use of the fibre fragmentation technique. In this way, the influence of fibre surface treatment,[1] the effect of fibre finish[2] and the effect of hygrothermal exposure[3] could be described fundamentally.

*One of a Collection of papers honoring Lawrence T. Drzal, the recipient in February 1994 of *The Adhesion Society Award for Excellence in Adhesion Science, Sponsored by 3M.*

The present knowledge about fibre/matrix bonding in carbon-fibre-reinforced plastics (CFRP) is not only based on single-fibre composite tests. Although the interlaminar shear strength test (ILS or short beam shear test) in principle is a poor test, *e.g.*, due to the complicated stress field in the specimen,[4] the test technique contributed much to the understanding of fibre/matrix bonding. With this technique, the influence of chemical interactions,[5] and different surface treatments, on the bond strength of high modulus and high tensile strength carbon-fibre-reinforced polymers[6,7] was successfully investigated. In recent years, it has been shown that other mechanical properties determined on multi-fibre composites (real laminates) more strongly reflect the quality of the fibre/matrix bond strength. This is, *e.g.*, demonstrated by Norita *et al.*,[8] who showed that the increase in transverse (90°) and in-plane shear strength (measured on $\pm 45°$ specimens), due to a fibre surface treatment, is 2–3 times larger than the increase of the interlaminar shear strength.

In the present work, attention is focussed on the transverse strength of (mainly) CFRP, and a procedure is described to deduce from the transverse strength a fibre/matrix bond strength. Before this can be done, different aspects of multi-fibre composites have to be treated due to their interaction with the fibre/matrix bond strength.

The importance of the fibre/matrix bond strength for the transverse strength can be made clear by the approach of Cooper and Kelly,[9] considering the extreme conditions:

(a) the fibre and interface are very strong and
(b) the interface is very weak.

In the latter case, fracture is caused by matrix failure in the plane of minimum distance between the fibres. Neglecting the influence of randomness of the fibre distribution, the transverse strength, σ_t, in the case of a weak bond, can be estimated by:[9]

$$\sigma_t \doteq \sigma_m\left(1 - \sqrt{\left(\frac{4V_f}{\pi}\right)}\right) \tag{1}$$

where σ_m and V_f are the ultimate tensile strength of the matrix and the fibre volume fraction, respectively. The transverse strength in the case of an imperfect interface with a strength $\sigma_i < \sigma_m$ is given by a "law of mixtures" relation

$$\sigma_t = \sigma_m\left(1 - \sqrt{\left(\frac{4V_f}{\pi}\right)}\right) + \sigma_i\left(\sqrt{\frac{4V_f}{\pi}}\right) \tag{2}$$

which leads, in the extreme case of perfect bonding, to $\sigma = \sigma_m$. According to this approach, the transverse strength of a composite with $V_f = 0.6$ is in the range $0.125\,\sigma_m \leq \sigma_t \leq \sigma_m$ when $0 \leq \sigma_i \leq \sigma_m$. This simple approach, showing the importance of the fibre/matrix bond, neglects many important aspects, so that refinements are necessary.

In the present work, an attempt is made to describe several of these aspects. The basis of the present approach is an experimental technique which considers the statistical nature of transverse cracking. Transverse cracking was studied in specimens cut out of 0/90/0 laminates, which, due to the higher fracture strain of the load carrying 0°-layers,

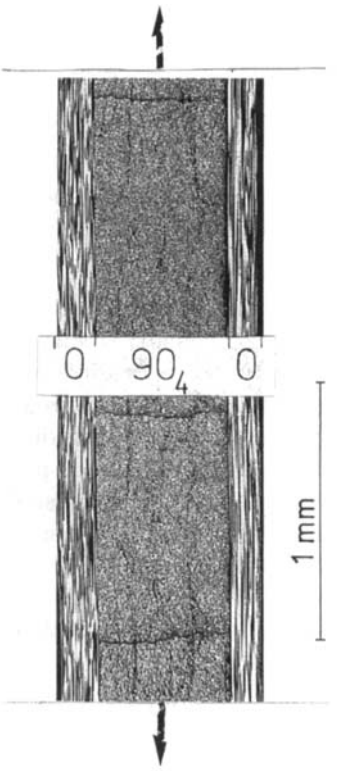

FIGURE 1 **Micrograph of the edge of a polish**ed CFRP $0/90_4/0$ laminate showing the phenomenon of multiple transverse cracking after tensile loading.

show multiple failure in the transverse layers before final failure occurs. As an example, Figure 1 shows three cracks in the transverse layer of a $0/90_4/0$ CFRP laminate. In the case of cross-ply laminate testing it is obvious to describe the strength of the transverse layer in terms of strain instead of stress. In the following, the findings based on this test technique described in the literature[10-20] are summarized.

EXPERIMENTAL TEST TECHNIQUE

In recent years, transverse cracking was investigated in several CFRP materials.[10-12,15,16] A detailed description of materials and experiments is given in the original references. Quasi-static tensile experiments were performed on cross-ply specimens 16 mm wide and 180 to 200 mm long leading to a specimen gauge length of 100 to 115 mm. During the displacement-controlled experiments (cross head displacement usually 2 mm/min) the load, the strain and the dynamic load change is measured and registered with a high-speed recorder or a transient recorder in combination with a computer. The strain is measured with an extensometer with a gauge length of 50 mm, whereas the dynamic load change is measured with a piezo-electric load cell.

Investigations of transverse cracking in crossply 0/90/0 laminates are attractive, as one test principally delivers as many data as cracks occur, whereas a test on a unidirectional specimen (transverse to the fibre direction) delivers only one result. To make use of the phenomenon of multiple cracking, two requirements have to be satisfied:

- the strain at which every single crack occurs must be measured
- the transverse ply must be divided into segments (elements), all of which can fail.

The first requirement is satisfied by making use of a piezo-electric transducer. This device registers dynamic load changes very accurately. A dynamic load drop occurs as the result of an unstable development of a crack. This crack leads to a small elongation of the specimen, which in turn gives rise to a small load drop in a displacement-controlled test. The thinner the transverse ply, the smaller the load drop. Further, cracks tend to grow more stably if the transverse ply is thin, so that the method usually gives good results for crossply CFRP with a transverse ply thickness of at least 0.5 mm (usually 4 plies). CFRPs with a thermoplastic matrix also show stable transverse crack growth, so that the method cannot be applied for these materials. The dynamic load drop measured every 0.001 second during a tensile test on a $0/90_4/0$ specimen is given in Figure 2a for a small time interval in which seven cracks occur. Figure 2b, with a higher resolved time scale, shows, for the first crack to appear, that an event of crack formation

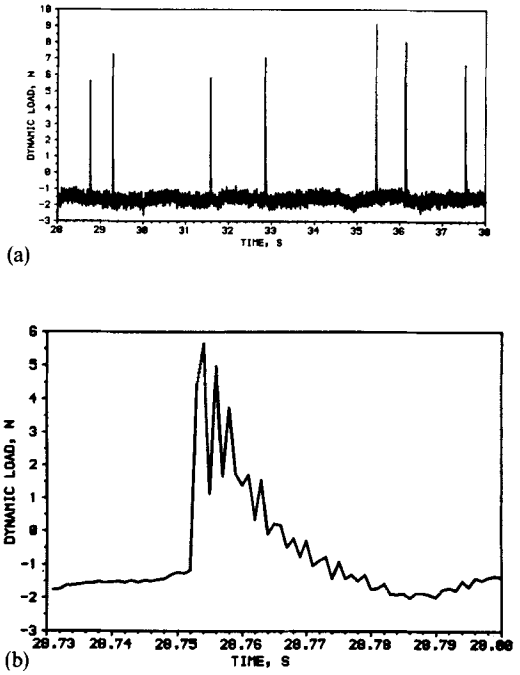

FIGURE 2 Piezo-electric signal as a function of the time during a tensile test on a $0/90_4/0$ (CG 43–750/HG 9106) specimen (Figure 2a) showing the first seven transverse cracks to occur and the first crack with a higher resolved time scale (Figure 2b).

leads to a dynamic load change lasting roughly 20 ms. If during this period another crack is formed, which is very unlikely, then this crack is not considered in the evaluation process. Differentiation of cracks occurring several milliseconds apart could be realized by considering the height of the load drop. This, however, was not attempted.

In order to be able to determine a statistical distribution of the transverse fracture strain, it is necessary to divide the transverse layer into a number of elements. The length of these elements is based on the distance from an existing crack over which the stress in the transverse layer recovers (see *e.g.*, Fig. 5). Several methods can be applied to determine this length. For the present technique, a shear-lag analysis is applied the details of which have been described before.[10, 20] According to this analysis, the stress in the interrupted transverse layer is reintroduced by shear stresses which are only active in the shear transfer zone, a zone of limited thickness between surface 0° and 90° layers. This shear-transfer layer was assumed to be a matrix-rich layer with the thickness of twice the fibre diameter. The stress in the transverse ply with a crack at $x = 0$ can be expressed by:

$$\sigma_{2,x} = \sigma_{2,\infty}(1 - \exp - (\gamma x)) \tag{3}$$

with

$$\gamma = \sqrt{\frac{G_m}{b} \cdot \left(\frac{1}{E_1 a_1} + \frac{2}{E_2 a_2}\right)} \tag{4}$$

in which $\sigma_{2,\infty}$ is the undisturbed stress in the transverse layer, E_1, E_2, G_m are the tensile moduli of the surface layer, transverse layer and the shear modulus of the matrix, respectively. The thicknesses of the transverse layer, surface layer and shear transfer zone are expressed by a_2, a_1 and b, respectively. The undisturbed stress consists of a thermal and a mechanical component. The thermal strain in the transverse layer of a 0/90/0 laminate is calculated with the aid of the thermal expansion coefficients in and perpendicular to the fibre directions,[10-12] with the aid of

$$\varepsilon_2^t = \frac{\Delta T(\alpha_2 - \alpha_1) E_1 a_1}{E_1 a_1 + E_2 a_2/2} \tag{5}$$

where ΔT is the difference between curing and test temperature and α_2 and α_1 are the thermal expansion coefficients, in the loading direction, of the transverse and longitudinal layers. The thermal expansion coefficients α_2 and α_1 can be determined experimentally with the aid of the deflection of an unbalanced laminate.

According to the applied shear-lag analysis, the maximum shear stress in the shear transfer zone at $x = 0$ follows from:

$$\tau_{max} = \frac{G_m}{b} \cdot \left(\frac{\sigma_{2,\infty}}{\gamma E_2}\right) \cdot \left(1 + \frac{E_2 a_2}{2 E_1 a_1}\right) \tag{6}$$

with γ given by Eq. (4).

The stress in the transverse layer close to an existing crack is small (according to Eq. (3)), so that in this area no further cracking will occur. This is the reason for the more or less regular crack spacing found in crossply laminates under different loading

conditions. The length of the elements is now somewhat arbitrarily chosen to be that length over which 90% of the undisturbed stress is reached. Substituting in Eq. (3) $\sigma_{2,x} = 0.9\ \sigma_{2,\infty}$ thus delivers half the element length $l_o/2$. Knowing the element length, the number of elements in the specimen free length is determined and a statistical distribution of the element fracture strain can be determined based on the crack data. This is possible after making the simplification that, when an element fails, the stress in the broken element is zero (so that the elements break only once) and that the stress in elements with broken neighbours is undisturbed. The strain at the respective element failures principally is determined by taking the sum of the measured average mechanical strain at the time of failure and the thermal strain determined with Eq. (5). The average strain measured with an extensometer with a gage length of 50 mm can, however, be considerably influenced by additional strains due to the formation of cracks. This is demonstrated in Figure 3, where, up to a mechanical strain of 0.94%, the stress-strain curve shows the typical non-Hookean behaviour of increasing stiffness at increasing strain. In the range of 0.77% to 0.94% the piezo-electric device registered ten cracks, the influence of which is not visible. This may partly be based on the fact that transverse cracking can occur outside the 50 mm gauge length of the extensometer, as the gauge length of the specimen is 100 mm. The first discontinuous strain increase at a strain of $\varepsilon_{av} = 0.94\%$ is the result of a cluster of six transverse cracks. The strain of unbroken elements should be taken from the virgin stress-strain curve. Above the load where a discontinuous strain increase occurs, this virgin stress-strain curve is estimated by the line representing the tangent modulus in the top of the range, where the stress strain behaviour is practically uninfluenced by the cracks. The fracture strain of elements breaking above $\varepsilon_{av} = 0.94\%$ is thus determined by taking the strain, ε_{un}, from the estimated undisturbed stress-strain curve at the load where the elements fail, as indicated in Figure 3. In the sample presented in Figure 3, up to the unloading level 70 cracks occurred.

The crack data are evaluated in this way with the aid of a computer and the final result is a list of cracks with the mechanical strain at which they occurred.

The transverse fracture data can be described very well with the aid of a two-parameter Weibull distribution in terms of strain. The probability of element failure at

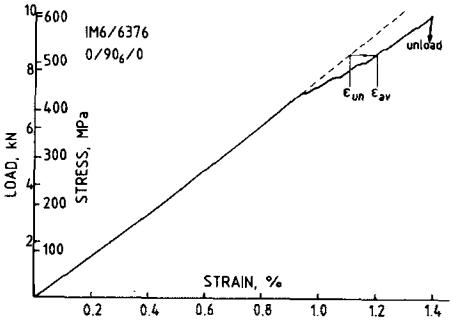

FIGURE 3 Stress-strain curve of a $0/90_6/0$ CFRP specimen to demonstrate the procedure to determine the virgin stress-strain curve.

a strain of $\varepsilon_{f,l_o}(=\varepsilon_{2,\infty})$ is given by

$$F = 1 - \exp - \left(\frac{\varepsilon_{f,l_o}}{\hat{\varepsilon}_{f,l_o}}\right)^a \tag{7}$$

in which "a" represents the shape parameter and $\hat{\varepsilon}_{f,l_o}$ the characteristic fracture strain ($\varepsilon_{f,l_o} = \hat{\varepsilon}_{f,l_o}$ at $F = 0.632$).

The probability of element failure for the elements is calculated with:

$$F = \frac{j}{N+1} \tag{8}$$

where j is the crack order number and N is the total number of elements in the specimen gauge length. The crack data are now transformed in pairs of values $\ln(-\ln(1-F))$ and $\ln(\varepsilon_{f,l_o})$ (ε_{f,l_o} = thermal + mechanical strain), and based on these data the Weibull shape parameter "a" and characteristic fracture strain $\hat{\varepsilon}_{f,l_o}$ are determined, making use of linear regression and least squares analysis. An example of a Weibull distribution[15] determined this way, with the aid of a single specimen tested at 40°C, is given in Figure 4. The crack data are described very well by the indicated two-parameter Weibull distribution (straight line). Due to the low test temperature, the thermal strain in the transverse ply is high ($\varepsilon_2^t = 0.552\%$) so that during mechanical loading up to a strain of 1.4% 169 elements out of 190 fail. It has been demonstrated[20] that, for larger crack densities (probability of failure $F > 0.2$), the probability of failure is reduced theoretically by the fact that the unbroken elements with broken neighbours effectively experience a lower stress, whereas above $F = 0.4$ to 0.5 the probability of failure increases again, due to the occurrence of multiple fracture in single elements. These deviations, however, were never observed in the actual data, probably because they are small in comparison with the scatter in the data.

The element length, l_o, based on 90% recovery of the undisturbed stress usually is a good choice for CFRP. The element length, in this case, is large enough to neglect the influence of non-homogeneous stresses and small enough to be able to neglect multiple failure of single elements. This was demonstrated with a Monte Carlo simulation of

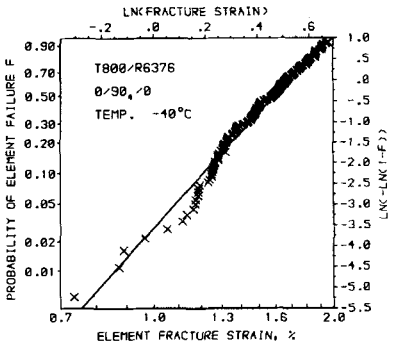

FIGURE 4 Weibull distribution for transverse cracking and transverse crack data for a $0/90_4/0$ specimen tested at −40°C (Ref. 15).

transverse cracking.[21] Transverse cracking was simulated with this technique, making use of experimentally-determined Weibull fracture strain distributions[10] according to the procedure described before (element lengths 0.69 to 1.12 mm, non-homogeneous stresses disregarded). For the simulation, 0.25 mm long elements were used, and the actual stress distribution in these elements was considered as a result of arbitrarily-distributed element failures. The results (number of cracks as a function of applied stress) were in good agreement with the experimental results of Reference 10.

Glass-fibre-reinforced plastic (GFRP) crossply laminates usually show, due to the lower transverse fracture strain, a number of cracks which is larger than the number of elements determined according to the present procedure. For this reason, the element length is reduced to half the size,[20] *i.e.*, the element is so long that with a crack in its middle the borders experience a stress of $\sigma_{2,x} = 0.684\,\sigma_{2,\infty}$.

In this case, a larger reduction of the probability of failure can be expected for larger crack densities, as elements with broken neighbours experience a clearly smaller stress than the undisturbed stress. Due to limited experience of the present technique with GFRP laminates, this could not be verified experimentally.

Transverse cracking in GFRPs (and AFRPs, *i.e.* aramid-fibre-reinforced plastics) is dominated by another aspect which reduces the probability of cracking more severely. This reduction is caused by the shear stress in the shear zone reaching the shear yield stress of the matrix or the interlaminar shear strength. Shear failure thus tends to occur if the fibre/matrix bond strength is low (*e.g.*, in AFRP), or if the modulus and/or thickness of the transverse layer (leading to high shear stresses, see Eq. 6) is large. GFRP with the isotropic glass fibre has a high modulus transverse to the fibre ($E_{\parallel} = 45$–50 GPa, $E_{\perp} = 14 - 17$ GPa[19] in comparison with $E_{\parallel} = 120$–160 GPa, $E_{\perp} = 8$–10 GPa for CFRP). The influence of this aspect is schematically demonstrated in Figure 5, which shows the shear stress distribution in the shear transfer layer and the tensile

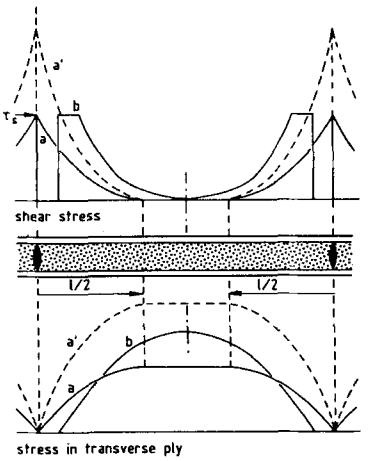

FIGURE 5 Shear stress in the shear transfer zone and tensile stress distribution in the transverse layer (schematic) near two transverse cracks in a cross-ply laminate. Curve *a* and *a'* linear-elastic and curve *b* with shear cracking and shear yielding. The applied stress in case of *a'* and *b* is twice as high as in case *a*.

stress distribution in the transverse layer near two transverse cracks. At a certain applied stress, the shear stress reaches the shear yield stress, τ_s (case a), and the tensile stress is practically completely recovered at a certain distance $l/2$ from the cracks. Doubling the applied stress theoretically leads to a doubling of the shear stress (case a'), and the undisturbed stress is again practically reached at a distance $l/2$ from the cracks. As the shear stress cannot acceed τ_s, shear yielding and eventually shear cracking occur (case b) leading to an increase of the ineffective length, *i.e.* that length on which the stress in the transverse ply practically completely recovers. Case b further represents a limit case, as the stresses (shear stress as well as the tensile stress in the transverse ply) will not be further increased on applying a higher stress. In this case, no further transverse cracking will occur, *i.e.* a saturation of cracking has taken place. This is the same condition reached in the final stage of the single-fibre fragmentation test. Thus, if saturation of transverse cracking occurs, the limiting shear stress (interlaminar shear strength) could be determined by a procedure similar to that for the single-fibre fragmentation test.

This condition of saturation of transverse cracking is closely approached during tensile tests performed on three specimens from an AFRP laminate $0/90_8/0$, as shown in Figure 6.[22] Specimen failure occurs when the probability of element failure reaches roughly $F = 0.7$ (indicating that 85 of 122 elements in the 105 mm gauge length have been broken).

The crack data influenced by the shear stress reaching its maximum value are not considered for the determination of the two-parameter Weibull distribution for transverse cracking. Principally, those crack data $\ln(-\ln(l-F))$, as a function of $\ln(\varepsilon_{f,l_o})$, are considered which contribute to a "linear" range of crack data which can be described by a single Weibull distribution. Thus, in the case of the data of Figure 6, only the first 25 cracks of every tested specimen are considered for the Weibull distribution.

With the aid of these Weibull distributions, transverse cracking in CFRP was investigated as influenced by the relevant parameters. In the next sections it will be shown that transverse cracking depends, *e.g.*, on the following parameters:

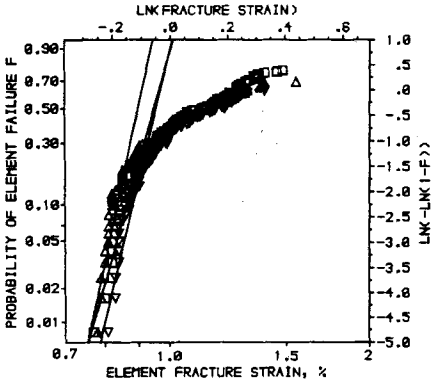

FIGURE 6 Transverse crack data and resulting Weibull distributions for transverse cracking (considering the first 25 cracks) for three $0/90_8/0$ AFRP specimens.[22]

- the defect distribution
- the fibre/matrix bond strength
- the constraining effect exerted by neighbouring plies.
- the strain magnification in the matrix.

These investigations on transverse cracking in CFRP have shown that transverse fracture can be described qualitatively with the aid of the following model.

MODEL FOR TRANSVERSE CRACKING

An important result from transverse cracking experiments is that the transverse strength or transverse fracture strain distribution of a CFRP lamina or laminate is *not* a material property. This is caused by the influence neighbouring plies exert on the strength or fracture strain distribution of a transverse layer. The real material property is the transverse fracture strain in the absence of defects, which in Figure 7 is represented by the perpendicular line ($a = \infty$, no scatter of fracture data). Fracture is caused by failure of the weakest of either the matrix or the interface (disregarding fibre splitting). In recent years, the composite research community has differentiated between interface and interphase. The interphase is the transition zone between the fibre and the bulk matrix, where the matrix properties gradually change from certain (mostly unknown) values near the fibre surface to those of the bulk matrix. Fracture, thus, can take place in the interface, interphase or in the bulk matrix. For ease of terminology, however, in the following sections fracture of either the matrix or the interface is mentioned with the intention that interface stands also for interphase.

The transverse fracture strain of a real material is reduced by the presence of defects, which results in a transverse fracture strain distribution with characteristic fracture strain $\hat{\varepsilon}_{f,l_o}$ and shape parameter "a", depending on the actual distribution of defects in terms of size and number. The correlation between defect size and transverse fracture strain is complicated by the influence of matrix ductility and the effect of constraint of

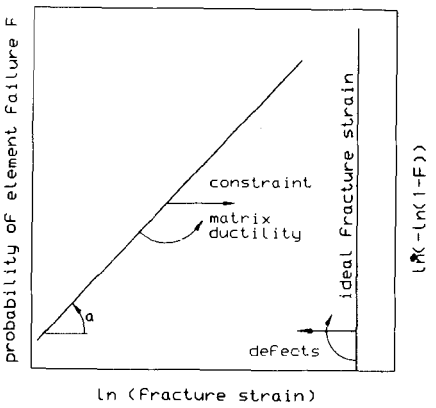

FIGURE 7 Model for transverse cracking in CFRP showing the influence of defects, matrix ductility and constraint on the Weibull distributions for transverse cracking.

neighbouring layers. Both factors tend to reduce the effectiveness of defects, thus try to shift the Weibull distribution backwards to the ideal fracture strain. The model, therefore, is qualitative due to unanswered questions, such as: what are the defects, what is their size and how effective are they in relation to the influence of ductility and constraint?

If we consider now an actual distribution of transverse cracks, *e.g.* that of Figure 4, then it is clear that the first cracks in the tail of the Weibull distributions occur in those elements containing the biggest defects. If we rise from the tail of this Weibull distribution to its top, then fracture of the respective elements is caused by smaller and smaller defects. In case the material is macro- and microscopically free of defects (voids), it can be assumed that the top of the Weibull distribution is dominated by intrinsic material properties (matrix or interface strength), whereas the bottom of the distribution is dominated by the defects.

As a final consequence of the model, a transverse strain at interface failure can be deduced assuming that the last breaking (strongest) element is defect-free. Its fracture strain thus represents the strain at which the weaker of either the matrix or the interface fails. As, usually, not all elements of the transverse layer fail, the fracture strain of the strongest element has to be determined by extrapolation of the Weibull distribution as shown schematically in Figure 8. The gauge length of the specimen usually contains 100 to 200 elements, so that the fracture strain of the strongest element (further in this work defined as the strain at interface failure) is calculated for the probability of failure, $F(= 100/101$ to $200/201)$, leading to the values of the hatched region in Figure 8. The model will be shown to describe the influence of several important parameters.

At this point, it is often argued that it should be demonstrated that the first crack occurs in the matrix, whereas the last occurring crack is an interface crack. This is, however, not the case. In both cases, the main part of the fracture surface is produced by an unstably (explosively) growing crack. The only difference is the nucleation area of the crack around the defect responsible for crack formation. These formation areas can

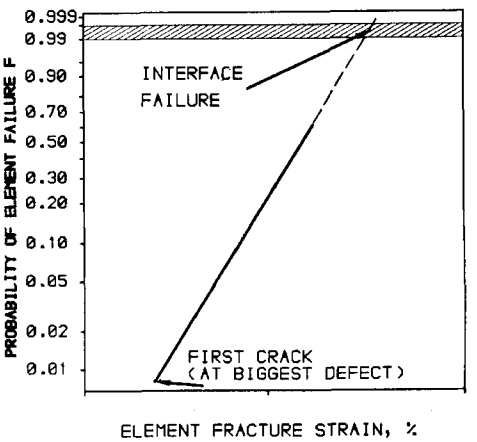

FIGURE 8 The strain at interface (or interphase) failure deduced from the Weibull distribution for transverse cracking.

probably be found in elaborative microscopical investigations, which, however, were not performed.

A certain degree of arbitrariness in the procedure followed to determine the strain at interface failure cannot be avoided. The last breaking element is, of course, not completely defect-free; a Weibull distribution of smaller transverse elements (*e.g.* 0.1 mm, if at all physically possible, instead of 0.7 mm as in the present case for elements of a 90_4-layer) would produce a higher strain at interface failure, as smaller elements statistically contain smaller defects. An alternative method to determine the strain at interface failure is a similar procedure applied on the Weibull distribution for transverse fracture of 3-point bending unidirectional specimens (*e.g.* for 1 mm thick, 16 mm long specimens). Although the volume of material tested this way is an order of magnitude larger than for elements in a crossply laminate, due to the stress gradient the effective volume tested under tension can be smaller.

THE INFLUENCE OF DEFECTS

Before discussing the influence of defects, a few remarks concerning defects have to be made first. In relation to transverse cracking, a clear description of possible defects cannot be given. In terms of size, the defects can be divided into defects on the macroscopic level (dimension of the prepreg ply thickness ≥ 0.1 mm) and on the microscopic level (dimension of the fibre diameter < 5–$10\,\mu$m). Macroscopic defects, *e.g.*, are voids, whereas microscopic defects can be dewetted or touching fibres. The influence of voids was (unintentionally) investigated on specimens produced from T800/6376 and IM6/6376 prepreg material. It was expected that these no-bleed prepregs with a smooth surface needed a lower autoclave pressure for consolidation. The stacked prepregs were covered by release fabric and a 5 mm thick aluminum plate to produce a smooth laminate surface. The selected autoclave pressure of 600 kPa, however, gave rise to macrovoid formation, non-homogeneously distributed in the

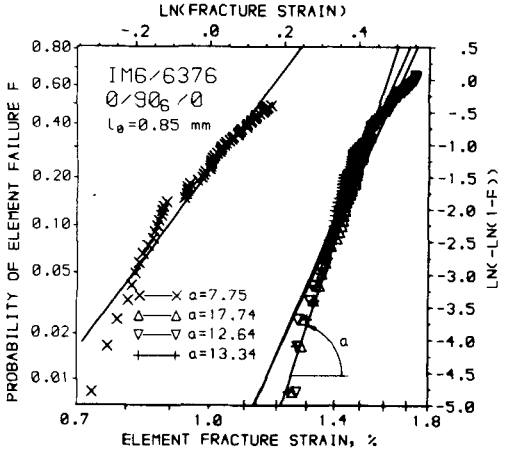

FIGURE 9 The influence of voids on the Weibull distribution for transverse cracking in one out of four specimens ($0/90_6/0$, IM6/6376) (Ref. 19).

laminate. Due to a local variation in thickness of the stacked plies, the pressure inside the stacked plies during consolidation was locally too low, resulting in the formation of voids. Transverse cracking was clearly influenced by the non-homogeneous distribution of these voids as demonstrated in Figure 9.

Three of four specimens show very similar transverse cracking behaviour, whereas the element fracture strains of the fourth specimen are clearly reduced due to the presence of the voids. The complete fracture data produced on $0/90_{12}/0$, $0/90_6/0$ and $0/90_4/0$ laminates for the systems IM6/6376 and T800/6376, and an extensive discussion of the results, can be found in Reference 12 and 19, respectively. Interestingly, it was found[19] that transverse cracking in GFRP is much less influenced by voids. This is probably caused by the magnitude of the strain magnification factor. This aspect will be discussed in a following section.

THE INFLUENCE OF CONSTRAINT

Early work on transverse cracking[22,23] revealed that the strength (or fracture strain) of a transverse ply increases if it is embedded between stiffer, *e.g.* 0°, plies. Further, it was found that this so-called effect of constraint increases if the thickness of the transverse ply decreases. This effect is schematically illustrated in Figure 10. The strain for the onset of transverse cracking increases if the thickness of the transverse lamina decreases. The strain at failure of the transverse laminate, however, does not increase. Although theoretically the latter should be the case, it was not measured experimentally. Another aspect of the influence of constraint is demonstrated in Figure 11, in which the Weibull distributions for fracture for the transverse layers 90_{12}, 90_6 and 90_4, embedded between 0° surface plies, are presented.[10] Apart from the fact that, in agreement with Figure 10, the transverse fracture strain (for the onset of cracking) increases at decreasing layer thickness, the Weibull shape parameter also increases at decreasing layer thickness. This means that the scatter in the fracture data decreases if the thickness of the transverse layer decreases.

The explanation of this phenomenon, presented before,[12] is based on the influence of stiff surface layers on the effectiveness of defects. Defects present in a range of unknown thickness close to the 0/90 interface are hindered from opening up and, thus, are

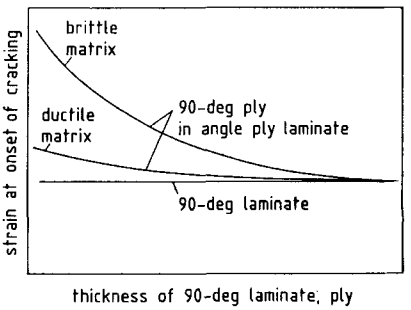

FIGURE 10 The influence of constraint on the transverse strength of CFRP with a brittle and a ductile resin system.

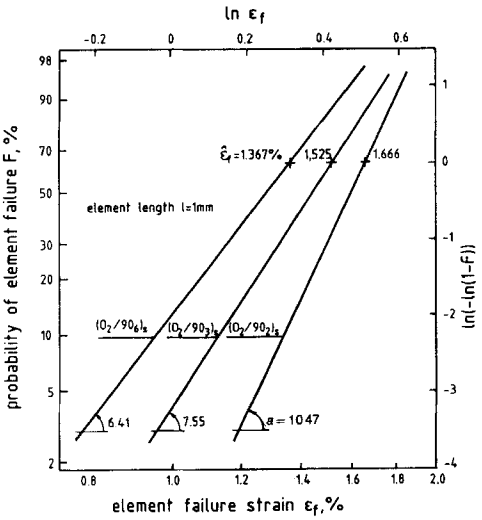

FIGURE 11 The influence of constraint on the Weibull distribution for transverse cracking in transverse layers differing in thickness. (Laminates $0_2/90_{12}/0_2$, $0_2/90_6/0_2$ and $0_2/90_4/0_2$, Material T300/914C) (Ref. 10).

hindered from growing due to the presence of the surface plies. Thus, the constraining effect has an influence similar to matrix ductility; it reduces the effectiveness of defects by reducing stress concentrations. Interestingly, the influence of constraint is large for CFRPs with brittle matrix systems but smaller for CFRPs with ductile matrix systems.[25] Thus, brittle matrix CFRPs reach a certain degree of quasi-ductility through the effect of constraint; if the matrix system is ductile on its own the influence of constraint is smaller as illustrated schematically in Figure 10.

Due to the effect of constraint, the thinner 90° layers embedded between stiffer layers *apparently* contain less defects (per unit volume). This causes the Weibull distributions *not* to shift in parallel, as would be the case if the effective defect distribution per unit volume were independent of the layer thickness, but to rotate to a steeper angle as shown in Figure 11.

A deterministic approach can only partly describe the increasing strength at decreasing transverse ply thickness. In many cases, the concept of strain energy release rate is used to explain the increase.[23,24] In this approach, the energy released by the specimen on the occurrence of a transverse crack is set equal to the energy necessary to produce this crack. This is not realistic, as a part of the energy released is dissipated in the specimen. In principle, the energy balance should be considered at that moment when the crack extending from a defect becomes unstable. Variations in transverse fracture strain or strength, on the basis of a constant transverse fracture toughness, can be predicted considering the non-homogeneous stresses due to cracks in the transverse ply as indicated in Figure 5. This approach was performed by Liu and Nairn[26] who made use of a variational approach to determine the stress distribution. They predicted a variation of the stress for transverse cracking in several CFRPs for crack densities larger than 0.2 cracks per mm.

The statistical aspect of transverse cracking as a result of the distribution of defects (flaws) in a fracture mechanical approach was performed by Wang[27] assuming a certain distribution of defects (flaws) in terms of number and size. A distribution of effective defects (called effective to describe on the macroscale the influence of micro-flaws) was placed symmetrically relative to the centre line of the transverse layer of crossply laminates. One distribution for a $0_2/90_6/0_2$, a $0_2/90_4/0_2$ and a second for a $0_2/90_2/0_2$ laminate was selected in such a way that the calculated stresses for transverse cracking were in agreement with experimental data. This promising approach should be further refined by distributing the defects also statistically in the thickness direction and by a complete integration of the physical nature of constraint into fracture mechanics.

THE FIBRE/MATRIX BOND STRENGTH

As outlined before, the strain at interface failure can be deduced from the Weibull distribution for transverse fracture. Assuming that the last breaking element is defect-free, the fracture strain of this element represents this material property. Its value is determined by extrapolation of the Weibull distribution to the value of the probability of failure, $F(=N/N+1)$. This procedure was followed for three different cases to determine the fibre/matrix bond strength as a function of

- transverse layer thickness
- test temperature
- level of fibre surface treatment.

It is obvious that the fibre/matrix bond strength, being a material property, should be independent of the thickness of the transverse ply. To demonstrate this, use is made of the Weibull distributions of Figure 11 discussed before. These Weibull distributions intersect in the upper right hand corner, indicating that a material property, the fibre/matrix bond strength, is approached for a high probability of failure, F. In the ideal case, the extrapolation of the three curves intersect in one point. Due to measurement inaccuracies, the assumptions made and material scatter, this is not the case. If the strain at interface failure is determined according to the procedure described before (for $F = 0.995$) this property varies from $\varepsilon_{int} = 1.75\%$ to $\varepsilon_{int} = 1.92\%$ by reducing the transverse layer thickness from 90_{12} to 90_4. Thus, a variation of a critical dimension (the transverse layer thickness) by a factor of 3 leads to a variation of the fibre/matrix bond strength of only 10%, which is an acceptable deviation.

The influence of the test temperature on transverse cracking and the fibre matrix bond strength was investigated on $0/90_4/0$ specimens produced from T800/6376 prepregs.[15] Tensile tests were performed in the temperature range of $-100°C$ to $+100°C$, and Weibull distributions for transverse cracking considering the actual thermal stresses were determined, for the test temperatures of $-100°C$, $-40°C$, RT, $+60°C$ and $100°C$. The test results were found to be influenced at increasing temperatures by:

- the ductility of the matrix
- the fibre/matrix bond strength.

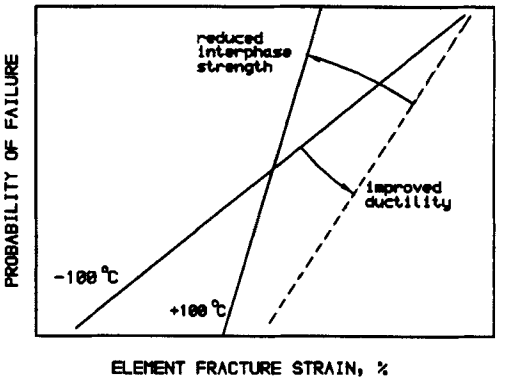

FIGURE 12 Influence of test temperature on the Weibull distribution for transverse fracture through improved matrix ductility and reduced fibre/matrix bond strength (Ref. 15).

As a result of these properties being influenced by the temperature, the Weibull distributions change, as indicated schematically in Figure 12 for the extreme temperatures of $-100°C$ and $+100°C$. The influence of the increasing temperature on the Weibull distribution for transverse fracture can be given with the aid of the model presented in Figure 7.

Remembering that the tail of the Weibull distribution is dominated by the defects and the top by the intrinsic material property (matrix fracture strain or strain at interface failure), the influence of the increasing temperature is twofold through the influence of ductility and matrix bond strength. At increasing temperature, ductility increases leading to a reduction of the effectiveness of the defects and, thus, to a shift of the bottom part of the Weibull distribution to higher fracture strains (dashed line in Fig. 12). Simultaneously, the fibre/matrix bond strength decreases at increasing temperature leading to a reduction of the transverse fracture strain, mainly in the upper part of the Weibull distribution. Thus, the final Weibull distribution for transverse cracking shows an increased strain for first ply failure but decreasing fracture strains for larger crack densities.

The strain for first ply failure (FPF, the first transverse crack), and the strain at interface failure determined for the different test temperatures, are indicated in Figure 13. A comparison with the thermal strain shows that at a test temperature of $-100°C$ the thermal strain is almost large enough to produce the first transverse cracks. The graph shows, further, that up to room temperature the improvement of matrix ductility leads to an increase for the FPF-strain. The severe reduction of the strain at interface failure above room temperature, however, completely overrules the positive effect of further increasing matrix ductility on FPF in this temperature range.

The influence of fibre surface treatment on transverse cracking, and the fibre matrix bond strength, was investigated with the aid of fibres subjected to different levels of a wet-oxidative surface treatment (IM fibre CG 43–750 of Courtaulds) embedded in the modified epoxy HG-9106.[16] The fibres were untreated (0% treated), 10%, 50% and 100% treated and sized (size designated size A). The strongest treatment (100%) represents the commercial wet-oxidative surface treatment.

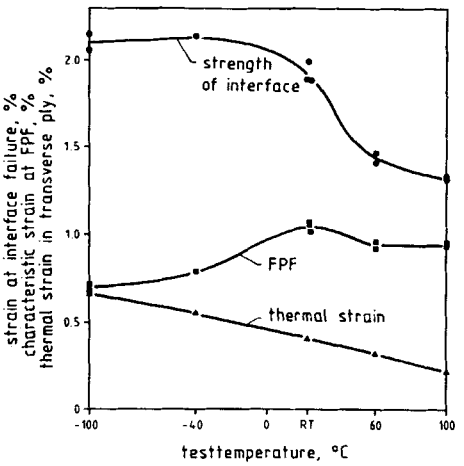

FIGURE 13 The total (thermal + mechanical) strain at first ply failure and at interface failure as a function of test temperature measured on $0/90_4/0$ CFRP specimens (T800/6376) (Ref. 15).

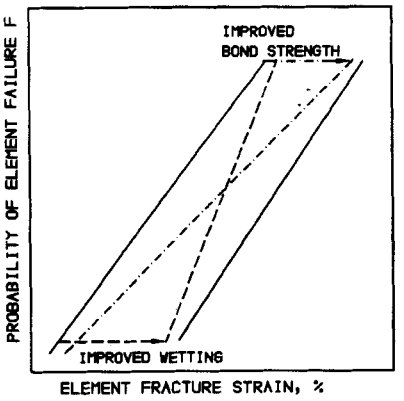

FIGURE 14 Influence of surface treatment on the Weibull distribution for transverse fracture through the reduced void content and the improved fibre/matrix bond strength (Ref. 16).

The influence of the surface treatment, discussed extensively together with the influence of cure temperature in Reference 16, is shown schematically in Figure 14. The surface treatment influences transverse cracking through the distribution of defects and the fibre matrix bond strength.

The surface treatment improved the wettability of the fibre, leading to a reduction of the void content of $V_v = 1.2\%$ for the untreated fibres in the modified epoxy to $V_v = 0.5\%$ for the 100% treated fibres. This reduced void content gives rise to a reduction of the number and size of defects. Its influence on the Weibull distribution, thus, is again explained with the aid of the model presented in Figure 7, which indicates that the reduction of defects leads to a shift of mainly the tail of the Weibull distribution to higher fracture strains, as shown schematically in Figure 14.

The main reason for the surface treatment, the improvement of the fibre/matrix bond strength, leads to a shift of the Weibull distribution mainly in the top part of the distribution. The ultimate result of both of these aspects of the surface treatment is, thus, a roughly parallel shift of the Weibull distribution to higher fracture strains.

STRAIN MAGNIFICATION FACTOR

Another important aspect in relation to transverse cracking is the strain magnification in the matrix, which is the result of the transverse modulus of the fibre being higher than that of the matrix. Assuming a square arrangement of the fibres, the strain magnification factor (*i.e.* the local maximum strain in the matrix divided by the applied transverse strain) can be estimated by:[28-30]

$$\mathrm{SMF} = 1/\left(1 - \left(1 - \frac{E_m}{E_{f,\perp}}\right)\sqrt{\frac{4V_f}{\pi}}\right) \tag{9}$$

in which E_m, $E_{f,\perp}$ are the matrix modulus and the modulus of the fibre in the transverse direction, respectively, and V_f is the fibre volume fraction. The strain magnification factor as a function of the fibre volume fraction is presented in Figure 15 for glass fibres ($E_{f,\perp} = 72\,\mathrm{GPa}$), carbon fibres ($E_{f,\perp} = 15\,\mathrm{GPa}$) and aramid fibres ($E_{f,\perp} = 5.4\,\mathrm{GPa}$) embedded in an epoxy resin ($E_m = 4.0\,\mathrm{GPa}$). Due to their high transverse stiffness, the isotropic glass fibres cause the largest strain magnification factor.

For a fibre volume fraction of $V_f = 0.65$, the strain magnification factor, *e.g.* measures SMF = 7.13, 3.00 and 1.31 for glass, carbon and aramid fibres, respectively, in a polymer matrix. The high strain magnification factor in GFRP explains the low transverse fracture strain of this material. The other extreme, a high transverse fracture strain for AFRP due to its low strain magnification factor is not measured, due to preliminary failure of the poor fibre/matrix bond (or transverse splitting of the fibre).

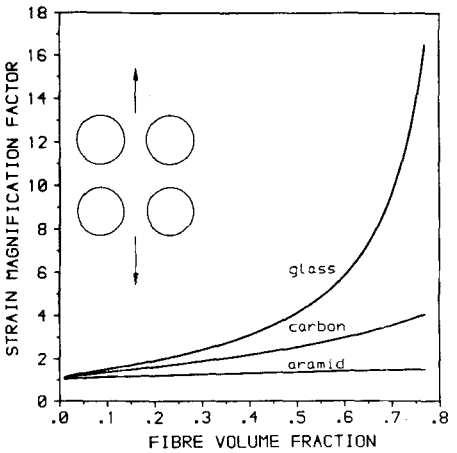

FIGURE 15 The strain magnification factor for a square array of glass, carbon and aramid fibres (Ref. 19) in an epoxy matrix.

Highest transverse fracture strains are reached for CFRP due to the moderate strain magnification factor combined with a good fibre/matrix bond.

It was mentioned before that voids considerably reduce the transverse fracture strain of CFRP; the influence on the transverse fracture strain of GFRP, however, is less. This difference must be considered in relation to the strain magnification factor. Pores of cylindrical shape produce in isotropic materials a stress concentration with a factor of 3. Thus, this stress concentration is of the size of the strain magnification factor in CFRP, but much smaller than the strain magnification factor in GFRP. Thus, transverse cracking in GFRP is probably dominated by the strain magnification factor and less by defects.

The estimation of the strain magnification in the matrix by Eq. (9) is based on a regular (square) distribution of the fibres. In real composites this distribution is more or less strongly irregular. The distance between the fibres varies, so that the strain magnification in the matrix between the fibres also varies. Therefore, the stress distribution on the microscopic level is unknown. Recent finite element investigations on the influence of matrix-rich zones, and different fibre packing arrangements, on the distribution of thermal stresses in fibre reinforced ceramics (SiC/LAS) show extremely varying stresses in the plane transverse to the fibres.[31] Nonhomogeneous thermal stresses are also present in fibre-reinforced polymers on which the non-homogeneous stresses due to transverse loading have to be superposed, resulting in complex stresses on the microlevel. Strain magnification factors calculated with, *e.g.*, Eq. (9) can, thus, only be a rough estimate of an average strain magnification for the average fibre volume fraction.

To study the influence of the average fibre volume fraction on transverse cracking in CFRP, $0/90_4/0$ laminates with fibre volume fractions of $V_f = 69\%$ to $V_f = 76.2\%$ were produced. The different fibre volumes were realized by making use of a different number of bleeder cloth layers (0, 1 and 2 respectively). The influence of fibre volume fraction on the unidirectional moduli, $E_\parallel$ and $E_\perp$, was determined experimentally on specimens cut from (0_6) laminates which were produced according to the same procedure. The results are indicated in Table I. Further, Table I shows the difference in thermal expansion coefficient between the transverse and longitudinal direction, $\alpha_2 - \alpha_1$ (calculated from the deflection of a strip of material from the three different laminates which occurs after grinding off one of the surface 0° plies). Based on these thermal expansion coefficients, the thermal strain in the transverse ply ε_2^t is determined. Finally, Table I contains the element lengths for the different laminates determined with the aid of Eq. (3), assuming that the shear transfer layer thickness for all laminates is twice the fibre diameter ($b = 0.010$ mm).

TABLE I
Fibre volume fraction and other data necessary for the determination and Weibull distributions of Figure 13

Fibre volume %	$0/90_4/0$ thickness mm	$E_\parallel$ GPa	$E_\perp$ GPa	$\alpha_2 - \alpha_1 \times 10^{-6}$ m/m/°C	ε_2^t %	l_o mm
69.0	0.79	156.4	8.62	36.46	0.509	0.559
73.3	0.74	165.9	9.37	31.63	0.440	0.564
76.2	0.71	171.0	9.78	28.65	0.398	0.567

The Weibull distributions for transverse cracking for three (of five) tested specimens determined according to the procedure described before are indicated in Figure 13. According to Eq. (9), the strain magnification factor rises from SMF = 3.47 to SMF = 3.98 on increasing the fibre volume from $V_f = 0.69$ to $V_f = 0.76$ (using $E_m = 3.6\,\text{GPa}$, $E_{f,\perp} = 15\,\text{GPa}$). The Weibull distribution for transverse fracture, thus,

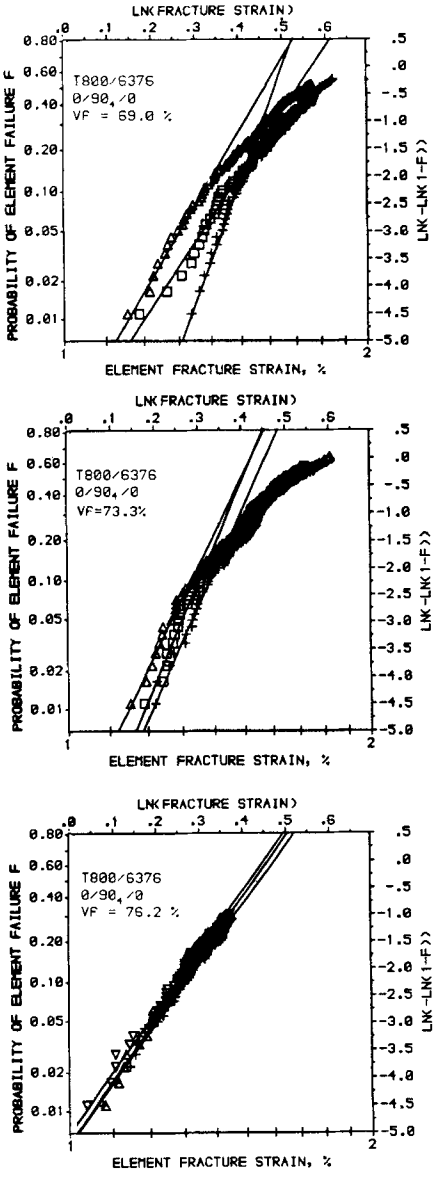

FIGURE 16 Influence of fibre volume fraction on the Weibull distribution for transverse fracture. (Laminates $0/90_4/0$, T800/6376).

should be shifted to fracture strains which are 15% lower, which is roughly confirmed by the results of Figure 16.

Several other aspects, however, also influence the Weibull distribution. Figure 16 clearly shows that the scatter in fracture data from specimen to specimen decreases at increasing fibre volume. This is probably the result of two phenomena. Firstly, a more homogeneous distribution of fibres is realized by compacting the material to a stronger degree. Secondly, on bleeding a part of the resin out of the stacked plies, voids are transported into the bleeder cloth leaving the compacted material with fewer, and a more homogeneous distribution, of defects. The scatter in the fracture data for $V_f = 0.69$ is somewhat larger than that of laminates produced from the same prepreg for another investigation.[15] The cause of the larger scatter is not known. Another difference with the latter investigation is the thermal strain, which was determined following a different procedure.

The specimens with the highest fibre volume fraction show a strong reduction of the strain at specimen failure, $\varepsilon_{max} = 1.0\%$ to 1.1%, in comparison with that of the other laminates, $\varepsilon_{max} = 1.3\%$ to 1.4%. This is probably caused by a reduction of the strength and fracture strain of the 0° plies if the fibre volume fraction becomes too high. The reduction of this failure strain causes the loss of the transverse fracture strain data above a total strain of $\varepsilon = 1.5\%$ (Fig. 16c). Due to the loss of these data points, the non-linear character of the fracture data visible in Figure 16a and 16b cannot be found in Figure 16c. This "non-linearity" is the result of a reduction of the probability of element failure at higher fracture strains, due to a reduction of the stresses in elements with broken neighbours as the shear yield stress (or interlaminar shear strength) is approached.

In the present approach, it was suggested that the shear-transfer layer is unaffected by the change in fibre volume fraction. This certainly is not the case. A "stiffening" of the shear transfer layer seems to be another source of a diminishing non-linear effect up to $\varepsilon_{f,l_o} = 1.5\%$ for the material with the highest fibre volume fraction.

In case the fibre/matrix bond strength is larger than that of the matrix, an attempt could be made to predict the transverse fracture strain if the strain magnification and the fracture strain of the matrix, ε_m, is known. The transverse fracture strain in this case simply follows from

$$\varepsilon_t = \varepsilon_m/\mathrm{SMF} \tag{10}$$

The fracture strain for the transverse ply of Figure 13a with $\varepsilon_m = 3.1\%$ and SMF = 3.5 thus should measure $\varepsilon_t = 0.9\%$. In reality, fracture strains of $1.1\% < \varepsilon_t < 1.9\%$ are measured.

The difference is based on:

- the strain magnification in the matrix varying locally as discussed before
- the fracture strain of the pure matrix is the result of a certain defect size which is typical for a pure resin specimen. A fibre-reinforced resin, due to the different processing, contains quite different defects, so that the fracture strain of pure resin is not comparable with the fracture strain of resin in which fibres are embedded
- the activated fibres (and in many cases the sizing) influence the properties of the surrounding matrix, leading to an interphase in which the properties (modulus, strength) differ from the bulk matrix. In Reference 18, *e.g.*, it was concluded that the

increase of fibre/matrix bond strength due to fibre surface treatment is partly due to the formation of a low modulus interphase with a high fracture strain.

Concluding, it must be stated that the stress field in transversely-loaded composites with statistically-distributed fibres is complex and has not been sufficiently investigated. In this stress field defects, the nature of which also is not sufficiently known, are active and dominate the onset range of transverse failure.

CONCLUSIONS

It has been shown that for CFRP a fibre/matrix bond strength (a strain at interface failure) can be deduced from Weibull distributions for transverse cracking. The procedure is based on a model which describes the influence of defects, matrix ductility and the effect of constraint exerted by neighbouring layers.

The validity of the method was demonstrated for transverse cracking influenced by

- transverse layers of different thickness
- the test temperature
- the surface treatment of the fibre.

One major drawback of transverse testing is the complex microscopic stress state due to the arbitrary distribution of the fibres. The severeness of the flaws, also non-homogeneously distributed, depends on the magnitude of the strain magnification, in the matrix. Due to the difference in strain magnification, flaws act differently in matrix systems with different fibres. This is the reason that the model and the fibre/matrix bond strength presented is only valid for CFRP.

References

1. L. T. Drzal, M. J. Rich and P. F. Lloyd, *J. Adhesion*, **16,** 1–30 (1982).
2. L. T. Drzal, M. J. Rich, M. F. Koenig and P. F. Lloyd, *J. Adhesion*, **16,** 133–152 (1983).
3. L. T. Drzal, M. J. Rich and M. F. Koenig, *J. Adhesion*, **17,** 49–72 (1984).
4. C. A. Berg, J. Tirosh and H. Israeli, *ASTM STP* **497,** 206 (1972).
5. E. Fitzer and R. Weiß, *Verbundwerkstoffe* (DGM, Oberursel, 1981), pp. 181–196.
6. E. Fitzer and H. Jager, *Zeitschrift für Werkstofftechnik*, **16,** 215–222 (1985) and 232–238 (1985).
7. E. Fitzer and H. Jager, *Haftung als Basis für Stoffverbunde und Verbundwerkstoffe* (DGM, Oberursel, 1987), pp. 135–160.
8. T. Norita, J. Matsui and H. S. Matsuda, in *Composite Interfaces*, Ed. H. Ishida and J. L. Ko (Elsevier Science Publ. Co, New York, 1986), pp. 123–132.
9. G. A. Cooper and A. Kelly, *Interfaces in Composites, ASTM STP* **452** (ASTM, Philadelphia, 1969), pp. 90–106.
10. P. W. M. Peters, *J. Comp. Mat.* **18,** 545–556 (1984).
11. P. W. M. Peters, *ASTM STP* **907,** 84–98 (1984).
12. P. W. M. Peters, *ASTM STP* **1012,** 84–99 (1989).
13. P. W. M. Peters, *Proc. Conf.*: "*Advancing with composites*", Milan, 673–689 (1988).
14. P. W. M. Peters, *Proc. European Symposium on Damage Development and Failure Processes in Composite Materials*, Leuven, 21–29 (1987).
15. P. W. M. Peters and S. I. Andersen, *J. Comp. Mat.*, **23,** 944–960 (1989).
16. P. W. M. Peters, *J. Comp. Mat.*, **28,** 507–525(1994).
17. P. W. M. Peters and H. Albertsen, *Proc.: Interfacial Phenomena in Comp. Mat.*, Leuven, 101–107 (1991).
18. P. W. M. Peters and H. Albertsen, *J. Mat. Sci.*, **28,** 1059–1066 (1993).
19. P. W. M. Peters and H. Meusemann, *Proc. ICCM VI/ECCM II*, London, 3.508–3.525 (1987).

20. P. W. M. Peters and T. W. Chou, *Composites*, **18,** 40–46 (1987).
21. S. Ochiai, P. W. M. Peters, K. Schulte and K. Osamura, *J. Mat. Sci.*, **26,** 5433–5444 (1991).
22. P. W. M. Peters, "Interface Dominated Mechanical Properties of Aramid/Epoxy", Report to AKZO (1988).
23. A. Parvizi, K. W. Garrett and J. E. Bailey, *J. Mat. Sci.*, **13,** 195–201 (1970).
24. D. L. Flaggs and M. H. Kural, *J. Comp. Mat.*, **16,** 103–116 (1982).
25. J. Varna and L. A. Berglund, *J. Comp. Tech. Res.* **13,** 97 (1991).
26. S. Liu and J. A. Nairn, *J. Reinforced Plastics and Composites*, **11,** 158–178 (1992).
27. A. S. D. Wang, in *Characterization, Analysis and Significance of Defects in Comp. Mat.*, Conference Proc. # 355, AGARD, 15.1–15.19, London (1983).
28. J. A. Kies, "Maximum strains in the Resin of Fiberglass Composites," NRL Report 5752 (1962) (Naval Research Lab., Washington, DC)
29. C. C. Charmis, *Comp. Materials*, Vol. **5,** *Fracture and Fatigue*, Ed. L. J. Broutman, (Academic Press, New York and London, 1974), pp. 94–153.
30. A. Puck, *Kunststoffe*, **55,** 913–922 (1965).
31. B. F. Sørensen, "Damage Mechanisms in Ceramic Matrix Composites", Thesis Technical Univ. of Lyngby, Denmark (1992).